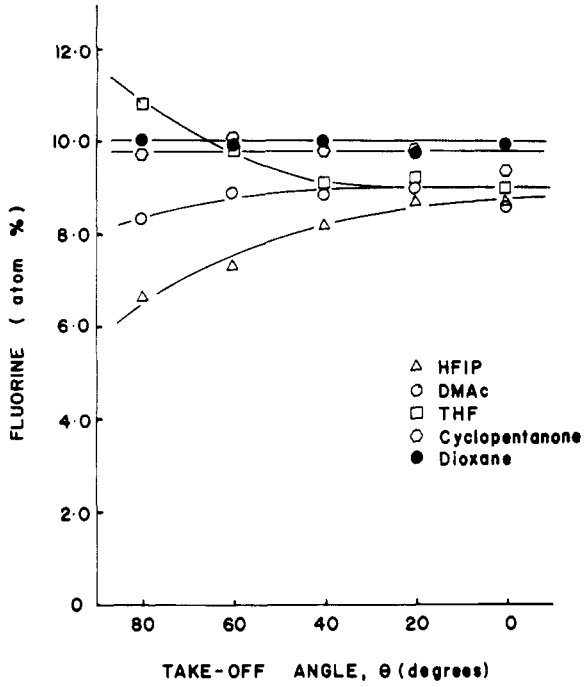

Figure 4. Casting solvent effect on the fluorine depth profile of PEU-1000-FP-24.

suggests that the soft segment has a lower surface energy than the hard segment.

The effect of casting solvent on the surface and bulk structure was studied for the PEU-2000-FP-23 and PEU-1000-FP-24 polymers, which can be prepared with a variety of good solvents. A remarkable linear correlation between the XPS composition data and the IR band ratios of bonded to nonbonded urethane carbonyls was obtained. This correlation provides direct evidence for the suggestion that the surface structure originates from the bulk structure. Also, when a very strong bulk-structure-perturbing solvent is used as a casting solvent, even the hard segment with a high surface energy can be enriched at the surface.

Acknowledgment. Support from N.I.H. grants HL25951 and RR01296 has made these studies possible. The editorial assistance of N. B. Mateo in the preparation of this manuscript is appreciated.

Registry No. (FB)(MDI)(PTMG) (block copolymer), 112666-66-7; (FP)(MDI)(PTMG) (block copolymer), 112666-67-8.

References and Notes

(1) Van Bogart, J. W. C.; Bluemke, D. A.; Cooper, S. L. *Polymer* **1981**, *22*, 1428.
(2) Leung, L. M.; Koberstein, J. T. *Macromolecules* **1986**, *19*, 706.
(3) Crystal, R. G.; Erhardt, P. F.; O'Malley, J. J. In *Block Copolymers*; Aggarwal, S. L., Ed.; Plenum: New York, 1970; pp 179–193.
(4) Yoon, S. C.; Ratner, B. D. *Macromolecules* **1986**, *19*, 1068.
(5) Abouzahr, S.; Wilkes, G. L.; Ophir, Z. *Polymer* **1983**, *23*, 1077.
(6) Thomas, H. R.; O'Malley, J. J. *Macromolecules* **1978**, *12*, 323.
(7) Skrovanek, D. J.; Painter, P. C.; Coleman, M. M. *Macromolecules* **1986**, *19*, 699.
(8) McLachlan, R. D.; Nyquist, R. A. *Spectrochim. Acta* **1964**, *20*, 1397.
(9) Klemperer, W.; Cronyn, M.; Maki, A.; Pimentel, G. *J. Am. Chem. Soc.* **1954**, *76*, 5846.
(10) Schrems, O.; Oberhoffer, H. M.; Luck, W. A. P. *J. Phys. Chem.* **1984**, *88*, 4335.
(11) Yoon, S. C.; Ratner, B. D. *Macromolecules*, preceding paper in this issue.

Infrared Dichroism Study of the Relaxation of Selected Segments along a Stretched Polymer Chain and Comparison with Theoretical Models

Jean Francois Tassin,* Lucien Monnerie, and Lewis J. Fetters

Laboratoire de Physicochimie Structurale et Macromoleculaire, Ecole Superieure de Physique et de Chimie de Paris, 10, rue Vauquelin, 75231 Paris Cedex 05, France, and Exxon Research and Engineering Co., Corporate Research Laboratories, Annandale, New Jersey 08801. *Received November 20, 1987*

ABSTRACT: The differences in chain relaxation as a function of segmental position along a deformed chain have been elucidated by studying linear isotopically labeled block polystyrenes. Films from three different copolymers have been stretched at constant strain rate and various temperatures. The orientation of the different blocks has been measured by infrared dichroism. End blocks appear to relax faster than the overall chain, the relaxation of which is still more rapid than that of the central block. The kinetics of the relaxation are sensitive to the length of the end block and the total molecular weight of the copolymer. The relative relaxation of chain ends with respect to the average orientation has been compared to the predictions of the Doi–Edwards model of chain relaxation. Good agreement has been obtained, without any adjustable parameter, when retraction, chain length fluctuations, and reptation processes have been considered.

I. Introduction

Recent molecular theories on the motion and the relaxation of polymer melts[1-4] have stimulated various experimental studies in order to test their validity. Many of them have been devoted to the viscoelastic behavior of entangled amorphous polymers in both the linear[5-9] and nonlinear domain.[10-14] Spectroscopic techniques like small-angle neutron scattering,[15-17] fluorescence polarization,[15,18,19] or infrared dichroism[20-24] have been used to directly study the behavior or relaxing deformed polymer chains on a molecular scale.

Molecular weight effects[21,23] or matrix influences[19,24] have already been studied and considered in the light of the Doi–Edwards (DE) molecular theory. A deeper testing of the basic processes of this model can be achieved by studying the relaxation of chain segments as a function of their location along the backbone by using isotopically labeled block copolymers. Indeed, the relaxation at long times is predicted to be nonuniform since two relaxation processes, the equilibration or retraction of the deformed

0024-9297/88/2221-2404$01.50/0

Table I
Names and Characteristics of the Isotopically Labeled Block Copolymers

	global characteristics of copolym		characteristics of deuteriated blocks			
copolymer	$\overline{M}_w$	$\overline{M}_w/\overline{M}_n$	no.	positn	$\overline{M}_w$	$\overline{M}_w/\overline{M}_n$
PS DH 184	184000	1.05	1	end	27000	1.03
PS HDH 188	188000	1.05	1	center	30000	1.03
PS DHD 500	502000	1.08	2	ends	38000	1.03

chain and reptation motion, lead to a faster relaxation of segments located toward the ends of the chain.

The first experimental results showing the main differences in the relaxation of the chain segments have already been reported.[24] This paper deals with a more complete study of the relaxation of a chain segment as a function of its position along the chain by using orientation measurements performed by infrared dichroism. More precisely, molecular weight effects have been studied. The relaxation of chain ends of different lengths will be compared to the relaxation of the average orientation and analyzed quantitatively in light of the DE model. Osaki et al.[25] have recently proposed an alternative method using rheooptical measurements. The present experiment offers the advantage of a direct determination of the relaxation of each block and can be applied to polymer melts instead of solutions. As we were preparing this paper, we learned that infrared dichroism on the same type of copolymers has also been used by another group[26] to study the relaxation of the central part of a chain. However, in that case only the orientation of the central part was measured, whereas we have been able to completely characterize the orientation of the chain.

II. Experimental Section

Samples. Three anionically polymerized block polystyrenes have been used in this study. Their description is given in Table I. Molecular weights of the initial homopolymers segments, diblocks and triblocks, were determined via size-exclusion chromatography where the μ-Styragel column set was calibrated by using a combination of the Polymer Labs and T.S.K. polystyrene standarts. A Waters 150C instrument was used with tetrahydrofuran as the mobile phase. The deuteriated part of the copolymers represents approximately 15% of the length of the chain. The copolymers called PS DH 184 and PS HDH 188 are of almost the same overall molecular weight and contain a deuteriated block of approximately the same length located either at the center or at one end of the chain, allowing an easy distinction between the behavior of the central part of the chain and the end segments. These two copolymers reveal the influence of the length of the end part of the chain by comparing the deuteriated end part (M_w = 27000) of PS DH 184 with the protonated end part (M_w = 78000) of PS HDH 188. The influence of the overall length of the chain on the relaxation of the end part can also be studied by comparing the behavior of the deuteriated end block of PS DH 184 with that of the PS DHD 500 copolymer.

Polymer films were prepared and stretched above the glass transition temperature at constant strain rate $\dot{\epsilon}$ as previously described.[22,24] The second moment of the orientation distribution function $P_2(\cos\theta)$, in which θ is the angle between the chain axis and the stretching direction has been measured by infrared dichroism using a Nicolet 7199 Fourier transform infrared spectrometer. The orientation of the hydrogenated blocks has been determined from the dichroism of the 906-cm^{-1} absorption band, assuming an angle between the normal of the benzene ring and the chain axis of 35°.[27] The orientation of the deuteriated blocks has been calculated by using the 2195- and 2273-cm^{-1} bands for which the following relations are valid:[24]

$$P_2(\cos\theta) = -3.8\frac{(R-1)}{(R+2)_{2195}} \qquad P_2(\cos\theta) = -2.7\frac{(R-1)}{(R+2)_{2273}}$$

where R is the dichroic ratio of the measured band. A mean value of $P_2(\cos\theta)$ obtained from these two measurements has been used to characterize the orientation of the deuteriated sequences.

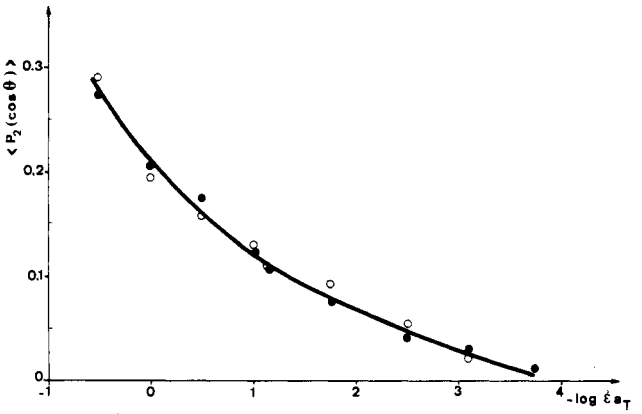

Figure 1. Master curve of the relaxation of average orientation for PS DH 184 (○) and PS HDH 188 (●) at a reference temperature of 120 °C.

Data Treatment. The samples were stretched at different draw ratios λ up to λ = 4 for various conditions of temperatures (T) and strain rates $\dot{\epsilon}$. The second moment of the orientation function was found to increase linearly with draw ratio whatever part of chain was observed. The orientation at a draw ratio of 4, which will be considered hereafter, was deduced from the best line over six different draw ratios. The average orientation has been calculated as the weight average of the orientation of each block.

Master curves for the relaxation of orientation were drawn subsequently from the data $P_2(\cos\theta)$ at λ = 4 obtained under different conditions of temperatures and strain rates, using the time temperature superposition principle. The reference temperature was 120 °C and the shift factor a_T was calculated from the equation[22]

$$\log a_T = \frac{-9.06(T-120)}{69.8+(T-120)}$$

Hereafter, only master curves will be considered.

III. Experimental Results

III.1. Orientation of the Copolymers PS HDH 188 and PS DH 184. The relaxation of the average orientation has been found to be almost identical for these two copolymers. This is depicted in Figure 1; the differences between the data points yield an estimate of the experimental accuracy.

The comparison between the relaxation of the orientation of the deuteriated end part of PS DH 184 and that of the overall chain is shown in Figure 2. The orientation of the deuteriated end block appears to be always lower than the average orientation but the relative splitting between these two curves increases at long times. This indicates that chain ends relax more rapidly than the overall chain, especially at long times. The smaller orientation of the end block at short times can be explained by the fact that no topological constraints are acting at the end of the chain to orient it. This behavior is similar to dangling chains in elastomeric networks.[28]

The nonuniformity of the relaxation along the chain appears even more clearly when the orientations of an end part and central part are compared. The behavior of the deuteriated end block of PS DH 184 is compared to that of the central deuteriated block of PS HDH 188 in Figure 3. At short times (for $-\log \dot{\epsilon} a_T < 1$) the relaxation of orientation is independent of the location of the segments along the chain; whereas at longer times, the end block relaxes much more rapidly than the central part of the chain, the orientation of which goes through a "plateau" for $2 < -\log \dot{\epsilon} a_T < 3$.

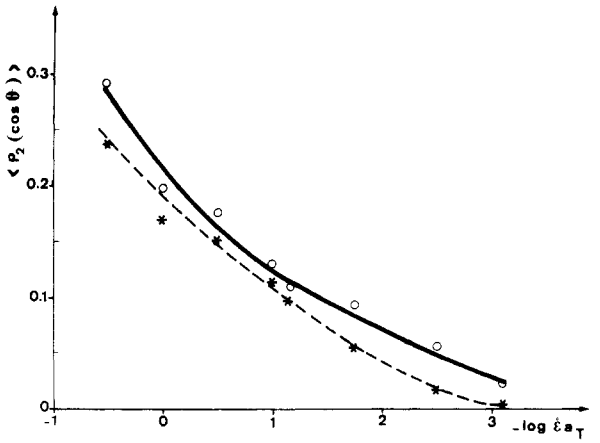

Figure 2. Comparison between the master curves of the relaxation of average orientation (○, full line) and that of the deuteriated end block (*, dashed line) for PS DH 184 at a reference temperature of 120 °C.

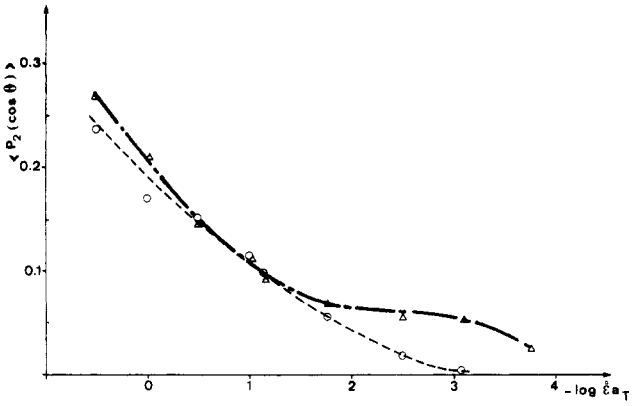

Figure 3. Comparison between the relaxation of the deuteriated end block of PS DH 184 (○, dashed line) and that of the deuteriated central block of PS HDH 188 (△, alternate line).

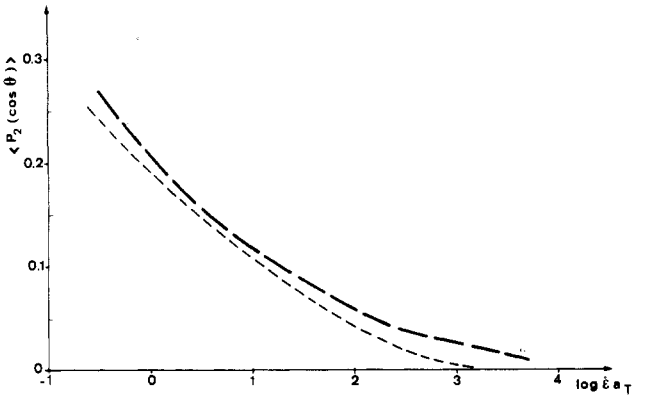

Figure 4. Comparison between the relaxation of the deuteriated end block of PS DH 184 (short dashed line) and that of the protonated end block of PS HDH 188 (long dashed line).

The influence of the length of the end part of the chain on its relaxation is depicted in Figure 4 where the relaxations of the end parts of M_w = 27 000 of PS DH 184 and of M_w = 78 000 are compared. The longer the end part, the slower the relaxation (at long times).

III.2. Orientation of the Copolymer PS DHD 500. The relaxation of the average orientation and that of the deuteriated end block is plotted in Figure 5. As in the previous case, the ends of the chain are less oriented than the overall chain, at both short and long times, but the relaxation of the end block appears more rapid especially at long times.

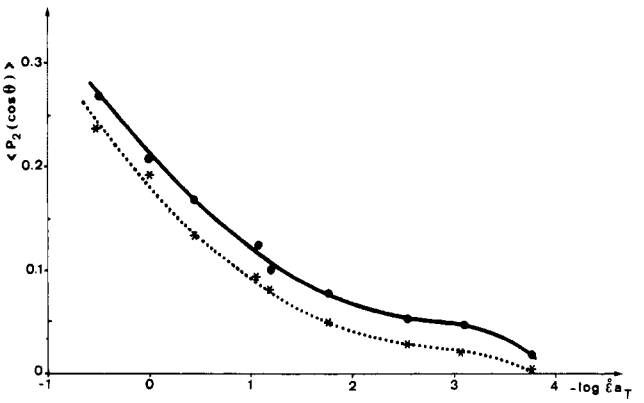

Figure 5. Comparison between the relaxation of average orientation (●, full line) and of deuteriated end block (*, dotted line) for PS DHD 500.

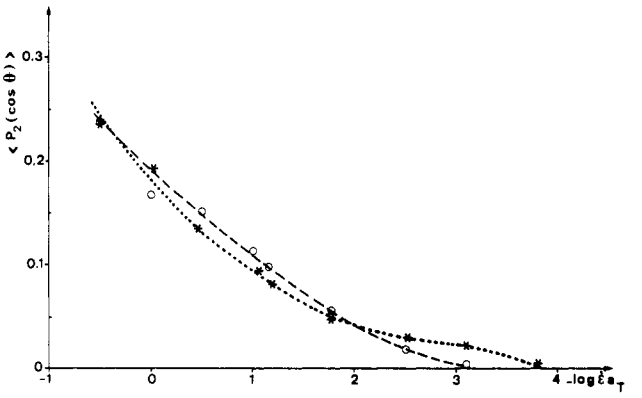

Figure 6. Comparison between the relaxation of the deuteriated end blocks of PS DH 184 (○, dashed line) and PS DHD 500 (*, dotted line).

The influence of the overall molecular weight on the relaxation of an end part is given in Figure 6 where the behavior of the deuteriated end blocks of the PS DH 184 and PS DHD 500 is plotted. It can be seen that the relaxation only differs at long times ($-\log \dot{\epsilon} a_T > 2$), where the end block belonging to the highest molecular weight chain relaxes slower.

These experimental results point out important differences in the kinetics of the relaxation of segments depending on their location along the chain. A faster relaxation of end segments has been evidenced, as well as noticeable influences of the length of the end block and the overall molecular weight of the chain.

In the next section, our attention will be focused on the molecular processes that might be at the origin of such behaviors, in the context of the DE model.

IV. Theoretical Predictions

IV.1. Qualitative Description. The relaxation of a stretched highly entangled chain is described according to the DE model through three different processes occurring on different time scales.

The first relaxation motion (designed by A hereafter) corresponds to a Rouse relaxation of a part of chain between two entanglements. This process is essentially local and its relaxation time τ_A is independent of the molecular weight of the chain. As a consequence of its local character, the kinetics of relaxation for this process are independent of the location of the segment along the chain.

The second relaxation process (B), characterized by a relaxation time τ_B scaling as the square of the molecular weight, is a retraction of the deformed chain inside its deformed tube to recover its equilibrium curvilinear length.

The retraction motion first takes place at the ends of the chain and diffuses toward the center. The relaxation is therefore no longer uniform along the chain. Nevertheless, when the curvilinear monomer density is constant and equal to its equilibrium value, i.e., at the end of this process, the orientation is constant along the chain and thus independent of the position of the segment.

The last relaxation motion corresponds to the reptation of the chain out of its deformed tube (C process) to reach an equilibrium isotropic configuration. The corresponding relaxation time (τ_C) scales as the third power of the molecular weight. As a basic assumption of this process, chain ends are assumed to loose their orientation as they leave the original deformed tube. Reptation therefore induces faster relaxation of chain ends.

To summarize, the DE model predicts that the relaxation is uniform along the chain at short times (A process) but not at longer times (B and C processes) where chain ends are expected to relax faster.

Several authors[4,7,29-34] have attempted to improve the DE theory by adding new processes.

A transition between the A process and the beginning of the retraction motion has been shown to be necessary,[7,31] corresponding to the so-called "equilibration across slip-links". This mechanism is a consequence of local differences in the curvilinear monomer density along the chain. The relaxation of orientation due to this process does not depend on the position of the segment.

On the time scale of τ_B, contour length fluctuations[29,32] induce a more rapid relaxation of chains ends. Indeed, wiggling motions involve forward and backward motions of the chains ends. Thus, chain length fluctuations destroy end parts of old tubes to create new isotropic ones. Ends of chains loose their orientation whereas centrally located segments remain unaffected. The DE model can also be improved by considering the relaxation of all the chains in a self-consistent way. The concepts of tube relaxation[30,31] and constraints release[3,32,34] imply a modification in the kinetics of the relaxation during respectively the retraction and the reptation stage. However, since topological constraints may disappear everywhere along the chain with the same probability, introduction of self-consistency should not change the *relative* relaxation of the segments along the chain. In a recent treatment, where an exact calculation instead of a mean-field theory was proposed, constraint release induced a larger effect on chain ends than on central segments.[34] The consequences of this treatment will not be discussed here.

This qualitative discussion shows that the processes of (i) retraction, (ii) chain-length fluctuations, and (iii) reptation induce a faster relaxation of chain end segments.

IV.2. Quantitative Evaluation of the Orientation of a Block. IV.2.1. Local Equilibration Process (A). The relaxation of orientation is independent of the location of the segment. Therefore, after averaging over all the chains, the orientation of the ith segment is identical with the average orientation, which has been already calculated:[22]

$$P_2^i(t) = P_2^{\text{network}}\mu_A(t) = P_2^{\text{network}}\left(1 + \sum_{p=1}^{N_R}\exp\left(\frac{-tp^2}{\tau_A}\right)\right) \quad (1)$$

where N_R is the average number of ROUSE subchains between entanglements. P_2^{network} represents the average orientation at the end of the A process, where we consider that the slip-link network is temporarily at equilibrium. In contrast with a previous work,[22] the comparison of the experimental data with the theoretical predictions avoids the determination of P_2^{network}.

IV.2.2. Chain Retraction Process (B). The evolution of average orientation during the retraction step is assumed to be directly proportional to the square of the curvilinear length of the chain:[22,30]

$$P_2(t) \propto L^2(t) \quad (2)$$

If only the orientation of the ith segment of the chain is considered, we can state that after averaging over all the chains

$$P_2^i(t) \propto \langle L_i^2(t)\rangle \quad (3)$$

The average orientation of a sequence containing N_D segments located between the αth and βth segments of the chain can be calculated as

$$P_2^D(t) \propto \frac{1}{N_D^2}\left(\sum_{i=\alpha}^{\beta} L_i(t)\right)^2 \quad (4)$$

where $L_i(t)$ is given by[3]

$$L_i(t) = L_{eq}\left[1 + (\alpha(\lambda) - 1)\sum_{p\,\text{odd}}\frac{4}{p\pi}\sin\left(\frac{ip\pi}{N_0}\right)\exp\left(-\frac{tp^2}{\tau_B}\right)\right] \quad (5)$$

in which L_{eq} is the curvilinear length of the chain at equilibrium, N_0 is the index of polymerization of the chain, and $\alpha(\lambda) = \langle|\mathbf{E}\cdot\mathbf{u}|\rangle_u$, $\mathbf{u}$ being a random unit vector and $\mathbf{E}$ the strain tensor. The proportionality constant in eq 4 can easily be calculated from the limiting behavior at short times. Two cases are of particular interest: (i) the central part of the chain is labeled; (ii) the ends of the chain are labeled.

Let f^D be the labeled fraction of the chain. In the case of a centrally labeled chain, transformation of the discrete summation of eq 4 by an integral and further integration from $\alpha = (1 - f^D)/2$ to $\beta = (1 + f^D)/2$ using expression 5 yields the following for the relaxation of the central block:

$$P_2^{\text{center}}(t) = \frac{P_2^{\text{network}}}{\alpha^2(\lambda)}\left[1 + \frac{\alpha(\lambda) - 1}{f^D}\times \sum_{p\,\text{odd}}\frac{8}{p^2\pi^2}(-1)^{(p-1)/2}\sin\frac{\pi p f^D}{2}\exp\left(-\frac{tp^2}{\tau_B}\right)\right]^2 \quad (6)$$

In the case of end labeling, if only one end is labeled (diblock copolymer), integration of eq 4 from 0 to f^D yields

$$P_2^{\text{end}}(t) = \frac{P_2^{\text{network}}}{\alpha^2(\lambda)}\left[1 + \frac{\alpha(\lambda) - 1}{f^D}\sum_{p\,\text{odd}}\frac{4}{p^2\pi^2}\times (1 - \cos\pi p f^D)\exp\left(-\frac{tp^2}{\tau_B}\right)\right]^2 \quad (7)$$

The case of a symmetrically end labeled copolymer is easily obtained by substituting f^D by $f^D/2$ in eq 7.

As expected, the relaxation of orientation due to the retraction process is related to the length and the position of the considered block along the chain. It can also be noted that, at long times, the orientation is again uniform along the chain $P_2^{\text{network}}/\alpha^2(\lambda)$.

IV.2.3. Chain Length Fluctuations. As quoted by Viovy,[32] chain length fluctuations may occur on the same time scale as the retraction motion. A terminal time approximation for the fraction of the chain still contained in the old tube at time t (i.e., not visited by a fluctuation) has been proposed[32]

$$f^{Fl}(t) = 1 - \rho(1 - \exp(-t/\tau_B)) \quad (8)$$

where $\rho = 1.47/N^{1/2}$, N being the number of entanglements per chain.

As chain length fluctuations occur, the end part of the chain that has left the initial tube at time t is assumed to have random orientation. Therefore, if only chain length fluctuations are considered (without retraction or reptation), the relaxation of the average orientation is given by

$$P_2^{av}(t) = P_2(0)f^{Fl}(t) \quad (9)$$

If chain length fluctuations are coupled with a retraction process, the average orientation can be expressed as the product of the two relaxation functions provide that the two mechanisms do not interact. The chain may later loose its remaining orientation by a reptation process so that the relaxation of the average orientation when retraction, chain length fluctuations, and reptation motions are considered is given by

$$P_2^{av}(t) = P_2(0)\alpha^{-2}(\lambda)g^2(t/\tau_B)f^{Fl}(t)\mu_C(t/\tau_C^{Fl}) \quad (10)$$

$g(t/\tau_B)$ is the relaxation function for the retraction process

$$g\left(\frac{t}{\tau_B}\right) = 1 + (\alpha(\lambda) - 1)\sum_{p\,odd}\frac{8}{p^2\pi^2}\exp\left(-\frac{tp^2}{\tau_B}\right) \quad (11)$$

μ_C characterizes the relaxation during the reptation stage

$$\mu_C(t) = \sum_{p\,odd}\frac{8}{p^2\pi^2}\exp\left(-\frac{tp^2}{\tau_C}\right) \quad (12)$$

and τ_C^{Fl} is the reptation time of the chain when chain length fluctuations are taken into account. This relaxation time can be related to τ_C the usual reptation time by the relation

$$\tau_C^{Fl} = \tau_C(1 - \rho)^2 \quad (13)$$

It is now necessary to calculate the relaxation of orientation of the ith segment of the chain for the chain fluctuation process. As a random orientation is expected if this segment has been visited by a fluctuation at time t, we write

$$P_2^i(t) = P_2(0)P^{Fl}(i,t) \quad (14)$$

where P^{Fl} designs the probability for the ith segment to have not been visited by a fluctuation at time t. With the lack of an exact mode distribution for chain length fluctuation, we calculate an approximate expression for the orientation of an end block as follows: at time t, the part of the chain that has been visited by fluctuations is $(\rho/2)(1 - \exp(-t/\tau_B))$. If a fraction f^D of the chain is labeled (at one end), its orientation will be assumed to be given by

$$P_2^D(t) = 0 \quad \text{for} \quad f^D < \frac{\rho}{2}\left(1 - \exp\left(\frac{-t}{\tau_B}\right)\right) \quad (15)$$

$$P_2^D(t) = P_2(0)\left(1 - \frac{\rho}{2f^D}\left(1 - \exp\left(\frac{-t}{\tau_B}\right)\right)\right) \quad \text{for} \quad f^D > \frac{\rho}{2}\left(1 - \exp\left(\frac{-t}{\tau_B}\right)\right) \quad (16)$$

A more detailed theoretical analysis of the mode distribution for this process is currently in progress in our laboratory.[35]

If retraction and reptation motions are also considered, the relaxation of orientation will be given by the product of the relaxation due to each mechanism.

IV.2.4. Chain Reptation Process (C). The orientation relaxes from the value at the end of the B process ($P_2^{network}/\alpha^2(\lambda)$) to 0. As in the previous treatments, we assume that a chain segment emerging from the original tube will take a random orientation. The orientation of the ith segment can be expressed as the product of the initial orientation, constant along the tube, by the probability that the segment has to be still trapped in the old tube at time t. This probability is given by the following expression:[1,2]

$$P(i,t) = \sum_{p\,odd}\frac{4}{p\pi}\sin\frac{p\pi i}{N_0}\exp\left(-\frac{tp^2}{\tau_C}\right) \quad (17)$$

If the orientation of a part of a chain of N^D segments located between the αth and βth segments is considered, one gets

$$P_2^D(t) = \frac{P_2(0)}{N^D}\sum_{i=\alpha}^{\beta}P(i,t) \quad (18)$$

In the case of a centrally labeled chain, the relaxation of the central block is given by

$$P_2^{center}(t) = \frac{P_2^{network}}{\alpha^2(\lambda)}\sum_{p\,odd}\frac{8}{p^2\pi^2}(-1)^{(p-1)/2}\sin\frac{\pi p f^D}{2}\exp\left(-\frac{tp^2}{\tau_C}\right) \quad (19)$$

As end labeling is concerned, the orientation of an end part of a diblock copolymer can be expressed as

$$P_2^{end}(t) = \frac{P_2^{network}}{\alpha^2(\lambda)}\sum_{p\,odd}\frac{4}{p^2\pi^2}(1 - \cos p\pi f^D)\exp\left(-\frac{tp^2}{\tau_C}\right) \quad (20)$$

The same relaxation functions for the orientation of central part and end part have been obtained by other authors in a different way.[36] When dealing with the reptation motion, it is interesting to establish the scaling law between the disengagement time τ_{dis}^{D,N_0} of a labeled end part of chain of length N_D on a chain of global polymerization index N_0. The curvilinear diffusion coefficient of the tube is $D_{tube} = D_1/N_0$, D_1 being a monomeric diffusion coefficient. The disengagement of an end part of length N_D is obtained when the chain has diffused over a distance L_D. Therefore

$$\tau_{dis}^{D,N_0} = \frac{L_D^2}{D_{tube}} = \frac{N_0 L_D^2}{D_1} \quad (21)$$

so that, finally

$$\tau_{dis}^{D,N_0} \propto N_0 N_D^2 \quad (22)$$

The disengagement time associated with a relatively short end part of chain can be much smaller than the overall reptation time, for instance two decades smaller for a end fraction of 10%!

V. Comparison with Experiments

V.1. Principle of the Comparison. It has been shown that the relaxation of orientation in constant strain rate experiments, measured at a given draw ratio, is very close to the relaxation following a step strain deformation of the same amplitude, as long as two types of experiments are related by $t = \dot{\epsilon}^{-1}$.[22] This avoids the use of cumbersome constitutive equations and has proven to be useful in the study of the average orientation. A similar procedure will be used here. The relaxation of orientation of the chain segments will be computed for a given draw ratio by using the above expressions, and correspondence between time and reciprocal of the strain rate will be assumed.

In this paper, we are mainly interested in the *differences* in the kinetics of relaxation of segments depending on their

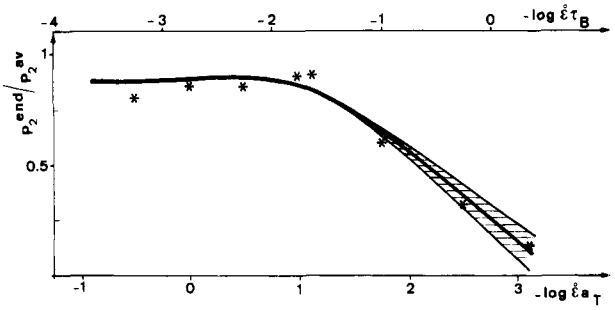

Figure 7. Relative relaxation of the deuteriated end block of PS DH 184 defined as orientation of the end block/average orientation. The shadowed region takes into account the uncertainty in the experimental data points.

location along the chain. It is therefore convenient to study the time evolution of ratios of orientation of blocks and average orientation. Such ratios clearly exhibit the differences in the relaxation. They can be calculated theoretically, assuming the existence of several relaxation processes, and might be compared to the experimental data. This offers two advantages. First, it avoids any rescaling parameter between experimental and calculated values of the orientation, and second, a local relaxation process having the same effect along the whole chain would not affect ratios of orientation. Important relaxation processes, like equilibration between slip-links (A′) or tube relaxation, can be omitted, since they do not modify the ratios of orientation, at least at the first order.

From these remarks, it appears that comparison between theory and experiments only requires the determination of one relaxation time at the reference temperature of the master curves. In a previous study, we determined τ_A = 5.6 s at 120 °C.[22] The same value will be used hereafter, the other relaxation times τ_B and τ_C being calculated from the theoretical scaling laws:

$$\tau_B = N^2\tau_A \quad \text{and} \quad \tau_C = 3N\tau_B \qquad (23)$$

Since an influence of the location of the segment along the chain is expected for times on the order of τ_B, the results will be presented as a function of log t/τ_B.

V.2. Relative Relaxation of Chains Ends. V.2.1. Behavior of PS DH 184. The faster relaxation of the deuteriated end block of this copolymer compared to the overall chain, already apparent in Figure 2, is clearly exhibited in Figure 7, where the ratio (orientation of the deuteriated end block over average orientation) is plotted versus $-\log \dot{\epsilon}a_T$ (lower axis) or versus $-\log \dot{\epsilon}\tau_B$ (upper axis). Chains ends and the overall chain are relaxing with the same kinetics up to times on the order of $10^{-2}\tau_B$. At longer times the relaxation of the end block is faster, inducing a decrease of the ratio. It can also be noted that the value of the ratio of orientations at short times is around 0.9. This can be interpreted as a "dangling-chain-like" effect of an extreme part of the end block. If we assume that at very short times the orientation (after averaging over all the chains) is uniform along the chain, a molecular weight of 3000 for the dangling unoriented part of chain is obtained. This value is much lower than the expected value of $M_e/2$ = 9000. The end of the chain seems to be sensitive to the anisotropy of the surroundings. To have an idea of the orientational coupling[37] acting on this chain end, we can assume that an end part of chain of length $M_e/2$ is affected by the interaction. Its orientation appears to be 0.7 times the orientation of the surroundings (a perfect coupling would yield 1).

The retraction, chain length fluctuation, and reptation processes qualitatively induce a more rapid relaxation of

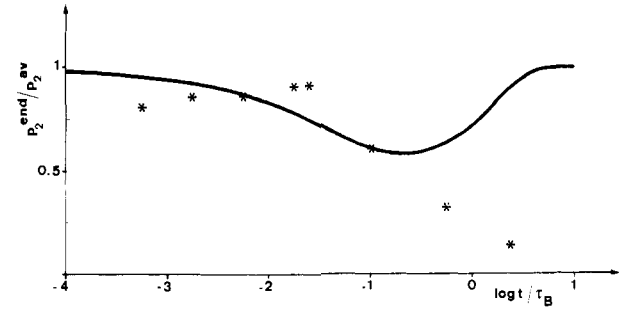

Figure 8. Comparison between the experimental relative relaxation of the deuteriated end block of PS DH 184 (*) and the predictions of the retraction process alone.

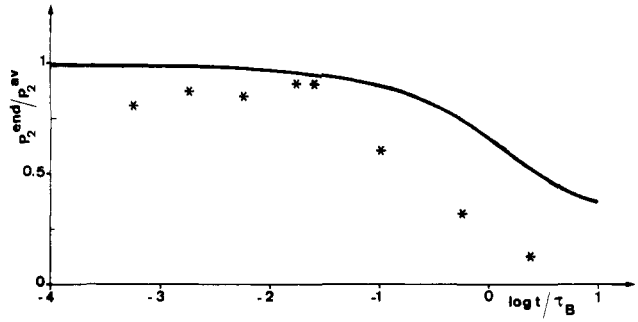

Figure 9. Comparison between the experimental relative relaxation of the deuteriated end block of PS DH 184 (*) and the predictions of the reptation process alone.

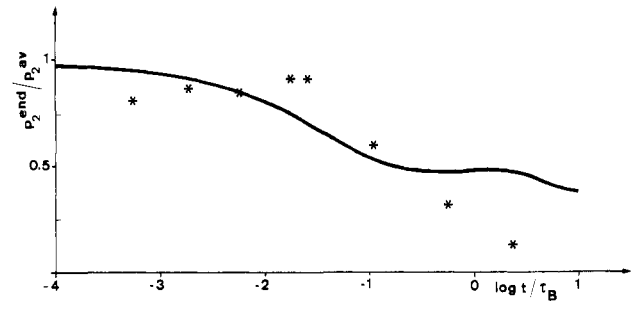

Figure 10. Comparison between the experimental relative relaxation of the deuteriated end block of PS DH 184 (*) and the predictions of the retraction and reptation processes.

chains ends. The theoretical evolution of the ratio (orientation of the end block over average orientation) will be calculated for the different processes and compared to experiment to check which motions are involved under our experimental conditions.

If retraction motion only is taken into account, the theoretical variation of the ratio of orientations with time is depicted in Figure 8. A minimum is observed for $t/\tau_B = 10^{-0.7}$. The limiting value of the ratio at short and long times is 1, since even at the end of the retraction process the orientation is constant along the chain. Experimental data are in agreement with the decrease occurring till $t/\tau_B = 10^{-2}$ but do not show any minimum in the expected time scale. It can be concluded that retraction cannot be considered separately.

The theoretical behavior predicted by the reptation process alone is presented in Figure 9. The ratio decreases smoothly for times larger than $10^{-1}\tau_B$. Experimentally, such a behavior is observed approximately a decade earlier. Therefore, reptation alone cannot account for the experimental observations. A process occurring at shorter times must also be considered.

It is now tempting to calculate the predictions of the retraction *and* the reptation processes. A better agreement

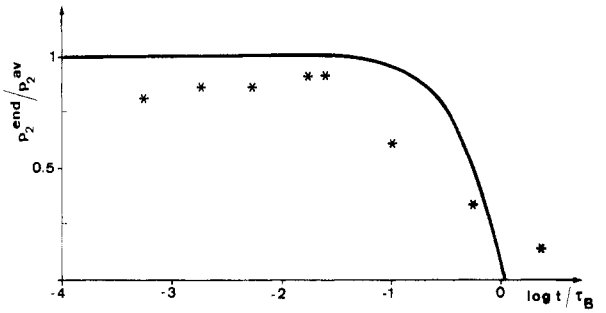

Figure 11. Comparison between the experimental relative relaxation of the deuteriated end block of PS DH 184 (*) and the predictions of the chain length fluctuation process alone.

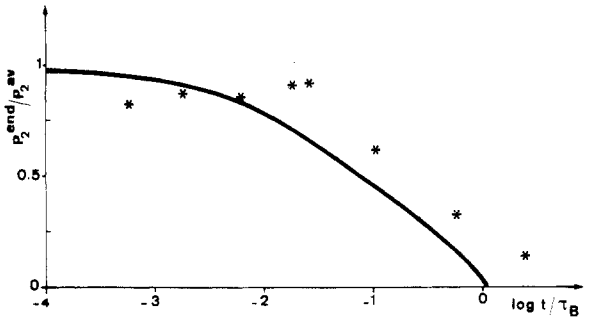

Figure 12. Comparison between the experimental relative relaxation of the deuteriated end block of PS DH 184 (*) and the predictions of the retraction, chain length fluctuation, and reptation processes.

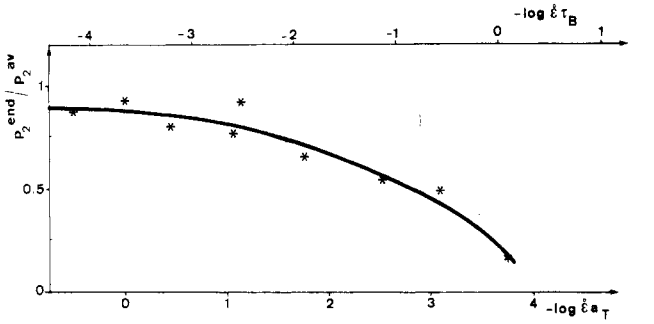

Figure 13. Relative relaxation of the deuteriated end block of PS DHD 500 defined as orientation of the end block/average orientation.

is obtained (Figure 10) but the predicted value of the ratio at times larger than τ_B lies above the experimental data, indicating the existence of an other relaxation process acting on this time scale.

The evolution of the same ratio calculated from chain length fluctuations (alone) is plotted in Figure 11. The terminal time approximation used in the treatment of this process induces a very rapid decrease of the ratio of orientations between $10^{-1}\tau_B$ and τ_B. This decrease is too fast compared to the experiment.

The theoretical variation of the ratio of orientations is given in Figure 12, for the case where retraction, chain length fluctuations, and reptation are taken into account. It can be seen that the decrease observed for $t > 10^{-2}\tau_B$ is somewhat more rapid than observed experimentally. The need to include the chain fluctuation process is evident but at the present time only a first-order approximation is available.

V.2.2. Behavior of PS DHD 500. This copolymer allows an examination of the relaxation of an end fraction (shorter than in the previous case, i.e., 7.5% of the total length instead of 15%) but belonging to a higher molecular weight chain. The evolution of the ratio (orientation of

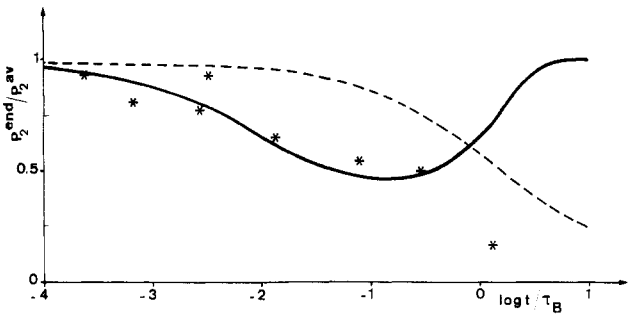

Figure 14. Comparison between the experimental relative relaxation of the deuteriated end block of PS DHD 500 (*) and the predictions of the retraction process alone (full line) and the reptation process alone (dashed line).

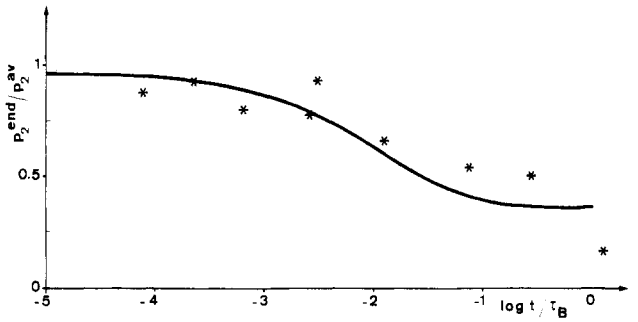

Figure 15. Comparison between the experimental relative relaxation of the deuteriated end block of PS DHD 500 (*) and the predictions of the retraction and reptation processes.

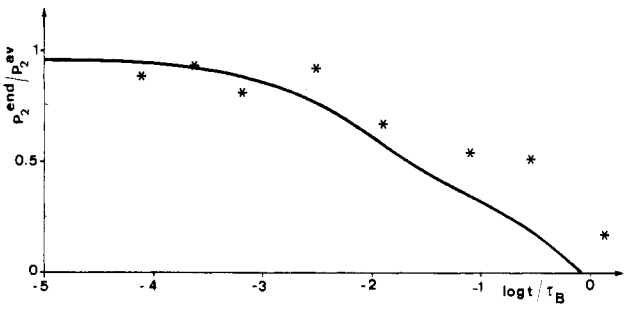

Figure 16. Comparison between the experimental relative relaxation of the deuteriated end block of PS DHD 500 (*) and the predictions of the retraction, chain length fluctuation, and reptation processes.

the end block/average orientation) is depicted in Figure 13. At short times, the deuteriated end block is less oriented than the overall chain. As previously, this can be interpreted by dangling-chain-like effects. The nonoriented extreme part would have a molecular weight of 3800, or the strength of the orientational coupling would be around 0.6. These values are on the same order of magnitude as those determined for the other copolymer. At longer times, a more rapid relaxation of the chain end segments can be seen from the decrease of the ratio of orientations.

As for the PS DH 184 block copolymer, the retraction motion predicts for the ratio of orientations as a function of time a curve showing a minimum for $t = 10^{-1}\tau_B$ which is not observed experimentally (Figure 14). The effect of the reptation process, reported on the same plot, is to induce a decrease in the ratio but at times too large compared to the data. If we now consider reptation and retraction processes, a rather satisfactory agreement is obtained (Figure 15), except for times on the order of τ_B where experiment indicates a smaller ratio than the theoretical predictions. Chain length fluctuations lead to a

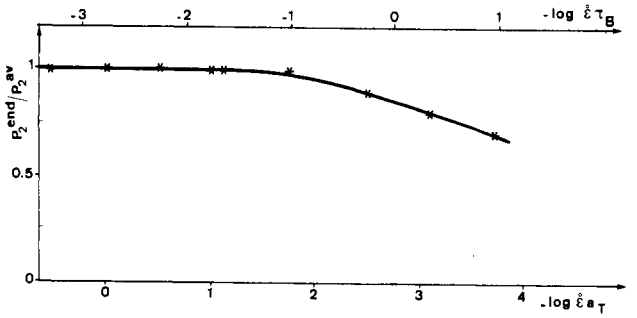

Figure 17. Relative relaxation of the protonated end block of PS HDH 188 defined as orientation of the protonated end block/average orientation.

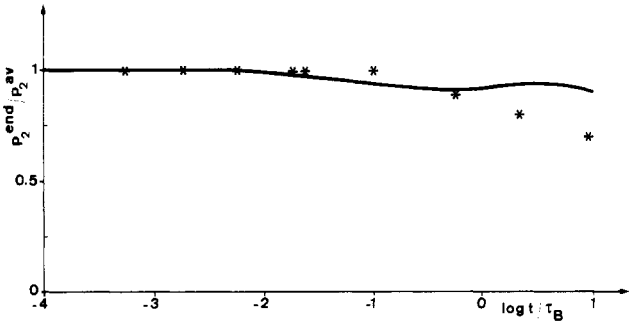

Figure 18. Comparison between the experimental relative relaxation of the protonated end block of PS HDH 188 (*) and the predictions of the retraction and reptation processes.

decrease in the orientation of the ends on the time scale of τ_B. Their effect, added to those of retraction and reptation, is given in Figure 16. The improvement due to this mechanism is apparent even if our present treatment overestimates its efficiency on the relaxation of chain ends.

V.2.3. Behavior of the PS HDH 188. This copolymer enables us to look at the influence of the length of the end block on its relaxation. The experimental behavior of the ratio of the orientation of the protonated end block over the average orientation is reported in Figure 17. Even if a larger end block is considered, the ratio always decreases on the time scale of τ_B but more moderately. The theoretical variation of this ratio, calculated by using the retraction and reptation processes, is given in Figure 18. Their influence appears in this case to be rather weak. Once more, divergence with the experimental data appears on the same time scale. If chain length fluctuations are also taken into account, the theoretical predictions are very close to the experiment Figure 19.

This comparison with the theoretical predictions of the various relaxation processes shows that, under our experimental conditions, the relaxation dynamics of the chain can be accounted for by a combination of retraction motion, chain length fluctuations, and the first stages of reptation.

V.3. Verification of the Scaling Law of the Disengagement Time of an End Block. The scaling law predicted in eq 22 can be tested by comparing the behavior at long times for the different end blocks, since we have shown that it was dominated by the reptation process. In Figure 4, the relaxation of the protonated end block of PS HDH 188 has been compared to that of the deuteriated end block of PS DH 184. An estimate of the ratio of the two disengagement times associated with these two blocks can be obtained from the distance between the relaxation curves at long times. Experimentally, the splitting is of 0.9 logarithmic time units, so the ratio of the disengagement times is approximately 8. Application of eq 23 yields

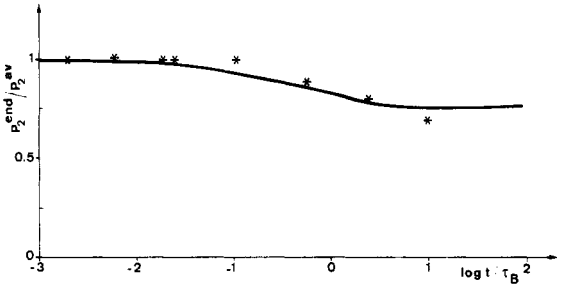

Figure 19. Comparison between the experimental relative relaxation of the protonated end block of PS HDH 188 (*) and the predictions of the retraction, chain length fluctuation, and reptation processes.

$\tau_{dis}^{79000}/\tau_{dis}^{27000} = 8.6$, which is in reasonable agreement with the experimental value, accounting for the N_D^2 variation.

The proportionality with the polymerization index can be checked by comparing the deuteriated end blocks of PS DH 184 and PS DHD 500. The relaxation of theses two blocks is reported in Figure 6. The ratio between the disengagement times can be estimated as 5.5, whereas the scaling law yields 5.4.

Since we are not able to measure directly the disengagement times, and taking into account the small number of data with regard to this scaling law, we do not claim that the foregoing constitutes a real test. Nevertheless, it has to be noted that our experimental results are compatible with its predictions.

Conclusion

Infrared dichroism performed on stretched films of isotopically labeled block copolymers of polystyrene has proven to be a powerful tool to study the orientation and relaxation of a selected part of a chain (center or end segments). The relaxation of orientation of a chain segment has been shown to depend on its location along the chain. The behavior of chain ends has been analyzed in light of the Doi–Edwards model. It has been shown that the relative relaxation of chain ends could be accounted for by the simultaneous considerations of the retraction, chain length fluctuation, and reptation processes. A satisfactory agreement was obtained for the three copolymers without any adjustable parameter. The behavior of an end block has been found to be sensitive to its own length and to the total length of the chain. The disengagement time associated with such an end block can be much smaller than the reptation time. The experimental data are in agreement with the theoretical scaling law, relating terminal segmental disengagement time to its length and to the overall length of the chain. A detailed analysis of the behavior of the central block is currently in progress.

Acknowledgment. We thank Drs. J. L. Viovy and M. Rubinstein for their interest in this work and fruitful discussions.

Registry No. PS, 9003-53-6.

Supplementary Material Available: Tabulated data on the orientation at $\lambda = 4$ of the different blocks in the various copolymers as a function of $-\log \hat{\epsilon}a_T$ for a reference temperature of 120 °C (2 pages). Ordering information is given on any current masthead page.

References and Notes

(1) de Gennes, P.-G. *J. Chem. Phys.* **1971**, *55*, 572.
(2) Doi, M.; Edwards, S. F. *J. Chem. Soc., Faraday Trans. 2* **1978**, *74*, 1789, 1802, 1818; **1979**, *75*, 32.
(3) Doi, M. *J. Polym. Sci., Polym. Phys. Ed.* **1980**, *18*, 1005, 2055.
(4) Graessley, W. W. *Adv. Polym. Sci.* **1982**, *47*, 67.

(5) Raju, V. R.; Menezes, E. V.; Marin, G.; Graessley, W. W.; Fetters, L. J. *Macromolecules* **1981**, *14*, 1668.
(6) Struglinski, M. J.; Graessley, W. W. *Macromolecules* **1985**, *18*, 2630.
(7) Lin, Y. H. *Macromolecules* **1984**, *17*, 2846; **1985**, *18*, 2779; **1986**, *19*, 159, 169; **1987**, *20*, 885.
(8) Watanabe, H.; Kotaka, T. *Macromolecules* **1984**, *17*, 2316; **1985**, *18*, 1008.
(9) Monfort, J. P.; Marin, G.; Monge, P. *Macromolecules* **1984**, *17*, 1551; **1986**, *19*, 393.
(10) Osaki, K.; Kurata, M. *Macromolecules* **1980**, *13*, 671.
(11) Vrentas, C. M.; Graessley, W. W. *J. Non Newt. Fluid. Mech.* **1981**, *9*, 339.
(12) Menezes, E. V.; Graessley, W. W. *J. Polym. Sci., Polym. Phys. Ed.* **1982**, *20*, 1817.
(13) Zebrowski, B. E.; Fuller, G. G. *J. Polym. Sci., Polym. Phys. Ed.* **1985**, *23*, 575.
(14) Tassin, J. F.; Thirion, P.; Monnerie, L. *J. Polym. Sci., Polym. Phys. Ed.* **1983**, *21*, 2109.
(15) Monnerie, L. *Faraday Discuss. Chem. Soc.* **1983**, *18*, 57.
(16) Boue, F.; Nierlich, M.; Jannink, G.; Ball, R. *J. Phys. (Les Ulis, Fr.)* **1982**, *43*, 137.
(17) Hadziioannou, G.; Wang, L. H.; Stein, R. S.; Porter, R. S. *Macromolecules* **1982**, *15*, 880.
(18) Fajolle, R.; Tassin, J. F.; Sergot, P.; Pambrun, C.; Monnerie, L. *Polymer* **1983**, *24*, 379.
(19) Tassin, J. F.; Monnerie, L. *J. Polym. Sci., Polym. Phys. Ed.* **1983**, *21*, 1981.
(20) Lefebvre, D.; Jasse, B.; Monnerie, L. *Polymer* **1983**, *24*, 1240.
(21) Lee, A.; Wool, R. P. *Macromolecules* **1986**, *19*, 1063.
(22) Tassin, J. F.; Monnerie, L. *Macromolecules*, in press.
(23) Lee, A.; Wool, R. P. *Polym. Prepr. (Am. Chem. Soc., Div. Polym. Chem.)* **1987**, *28*, 334.
(24) Tassin, J. F.; Monnerie, L.; Fetters, L. *J. Polym. Bull.* **1986**, *15*, 165.
(25) Osaki, K.; Takatori, E.; Kurata, M.; Ohnuma, H.; Kotaka, T. *Polym. J.* **1986**, *12*, 947.
(26) Lee, A.; Wool, R. P. *Macromolecules* **1987**, *20*, 1924.
(27) Jasse, B.; Koenig, J. L. *J. Polym. Sci., Polym. Phys. Ed.* **1979**, *17*, 799.
(28) Treloar, L. R. G. *The Physics of Rubber Elasticity*; Oxford University Press: London, 1958.
(29) Doi, M. *J. Polym. Sci., Polym. Lett. Ed.* **1981**, *19*, 265; *J. Polym. Sci., Polym. Phys. Ed.* **1983**, *21*, 667.
(30) Viovy, J. L.; Monnerie, L.; Tassin, J. F. *J. Polym. Sci., Polym. Phys. Ed.* **1983**, *21*, 2427.
(31) Viovy, J. L. *J. Polym. Sci., Polym. Phys. Ed.* **1985**, *23*, 2423.
(32) Viovy, J. L. *J. Polym. Sci., Polym. Phys. Ed.* **1986**, *24*, 1611.
(33) Viovy, J. L. *J. Phys. (Les Ulis, Fr.)* **1985**, *46*, 847.
(34) Rubinstein, M.; Helfand, G.; Pearson, D. S. *Macromolecules* **1987**, *20*, 822.
(35) Viovy, J. L., unpublished results.
(36) Lawrey, B. D.; Prudhomme, R. K.; Koberstein, J. T. *J. Polym. Sci., Polym. Phys. Ed.* **1986**, *24*, 203.
(37) Erman, B.; Jarry, J. P.; Monnerie, L. *Polymer* **1987**, *28*, 727.

Nuclear Magnetic Resonance Studies of Cutin, an Insoluble Plant Polyester

Tatyana Zlotnik-Mazori and Ruth E. Stark*

Department of Chemistry, College of Staten Island, City University of New York, Staten Island, New York 10301. *Received October 13, 1987*

ABSTRACT: High-resolution ^{13}C NMR studies have been conducted for cutin, a biopolyester that forms the structural component of the protective cuticle in terrestrial plants. With use of cross polarization–magic angle spinning (CPMAS) methods, the cutin structure is found to include methylene, methine, alkene, arene, keto, and ester functional groups. In addition, several types of mobile aliphatic carbons are observed by direct polarization (DP) methods. Estimates of the relative composition of each carbon type are also available from appropriate comparisons of CPMAS and DPMAS spectra. A combination of ^{13}C T_1, ^1H $T_{1\rho}$, and line-width measurements suggests that cutin is a moderately flexible netting, with motional constraints at particular cross-link sites. A preliminary structural model is proposed to account for the compositional and dynamic information obtained from ^{13}C NMR experiments.

Introduction

Higher plants are encased in a cuticle that serves both as a protective barrier to the environment and as a regulator of molecular diffusion among various organs. Cuticular breakdown may occur through the action of pathogenic fungi, with potentially devastating agricultural and economic losses. Yet paradoxically, cutin's susceptibility to degradation by mammalian enzymes may also facilitate digestion of many waste materials that could be fed to livestock.[1,2]

In aerial organs of terrestrial plants the cuticle consists of a waxy lipid waterproofing and the cutin polyester structural component. Although this latter material has several known hydroxy, epoxy, and phenolic fatty acid constituents (Figure 1), the insolubility of the polymer has hampered investigations of how its monomeric units are linked together.

For polymers and biopolymers, detailed structural information has become available routinely from solid-state nuclear magnetic resonance (NMR) and from the cross polarization–magic angle spinning (CPMAS) technique in particular.[4,5] Maciel and co-workers have used ^{13}C NMR to examine molecular alterations that accompany wood processing treatments and to isolate spectral contributions from lignin and cell walls in a variety of herbage samples.[6] More recently, Lewis et al. have deduced chemical bonding information from ^{13}C NMR spectra of both synthetic and natural lignins.[7,8] For polyester copolymers (Hytrel elastomers), Jelinski, et al. have elucidated the dynamic behavior at each backbone site of the hard and soft segments by combining ^{13}C and ^2H techniques and evaluating the effects of spinning, cross-polarization, and nuclear relaxation on various chemical moieties.[9-11] Though these examples focus on materials related to plant cuticle, numerous other solid-state NMR investigations of polymers and biopolymers have been conducted.[4,5,12]

We report herein the first high-resolution ^{13}C nuclear magnetic resonance studies of intact cutin. Cross polarization–magic angle spinning (CPMAS) with high-power proton decoupling has been employed in order to identify and estimate the relative numbers of magnetically distinct carbon moieties. In addition, several types of mobile carbons have been observed by combining traditional direct signal acquisition with low-power decoupling and

0024-9297/88/2221-2412$01.50/0